

## **Chapter III**

# **Tropical Pacific SSTA and Equatorial Westerly Wind Events**

### **III.1 Introduction:**

This chapter examines global statistical relationships between westerly wind events (WWEs) and sea surface temperature anomaly (SSTA) variability, using a compositing technique for the period 1986-1998. I describe the extent to which equatorial WWEs are associated with central and eastern equatorial Pacific waveguide warming and with local SSTA changes under the WWE. The work described in this chapter will appear in a forthcoming issue of the *Journal of Climate* (Vecchi and Harrison, 2000 - henceforth VH00), and builds on the WWE identification scheme outlined in Chapter II. The goal is to quantify the extent to which equatorial WWEs are fundamental to the onset and maintenance of warm El Niño/Southern Oscillation (ENSO) conditions. In order to understand the effect of WWEs on SSTA evolution, I begin by examining how SSTA changes in the absence of equatorial WWEs. I find that SSTA tends towards climatology in the absence of equatorial WWEs, whether the eastern equatorial Pacific has close to normal SSTA or warmer than normal SSTA.

There are significant SSTA changes under the main WWE wind anomalies for all three equatorial WWE types. The two equatorial WWE types whose main surface wind anomalies are west of the dateline (W and C) are associated with weak local surface cooling. The equatorial WWE type that has equatorial westerly wind anomalies east of the dateline (E) is associated with weak warming under those anomalies, when the eastern equatorial Pacific SSTA is close to normal.

When the tropical Pacific has near normal eastern equatorial Pacific SST, each of the equatorial WWE types are followed by substantial equatorial waveguide warming in the

central and eastern Pacific (composite warming as large as  $1.0^{\circ}\text{C}$ ); also more than 50% of the large amplitude WWEs were followed by NIÑO3 SSTA warming in excess of  $0.5^{\circ}\text{C}$ . These changes are of similar amplitude and spatial structure as those seen in the onset of El Niño, and are consistent with the predicted oceanic response to WWE forcing. When the eastern equatorial Pacific is initially warmer than usual, the two westernmost equatorial WWE types (W and C) are associated with the maintenance of warm El Niño eastern and central Pacific SSTA; these warm anomalies tend to disappear in the absence of those WWE types. The main result of this work is that WWEs, or some mechanism strongly correlated with WWEs, represent a fundamental process for waveguide warming in the onset of El Niño, and for eastern and central Pacific warm SSTA maintenance during El Niño.

Linear theory predicts that equatorial westerly wind anomalies in the western and central Pacific will drive current and temperature changes across the tropical Pacific through the excitation of eastward propagating Kelvin pulses (Godfrey 1975, Anderson and Gill 1976, McCreary 1976, Moore and Philander 1977, Giese and Harrison 1990). These Kelvin pulses will generally be associated with eastward surface currents, and warming of the surface ocean through anomalous advection of the background zonal temperature gradient. The first two vertical modes will generally lead to thermocline deepening, and subsequent surface warming due to vertical advection of anomalously warm sub-surface water. The details of the background ocean temperature and density field, and the structure of the wind forcing determines the details of the expected response. Though the first baroclinic mode is the one generally discussed, modes higher than the first are a significant part of the predicted linear response (Harrison and Giese 1989, Giese and Harrison 1990).

Modeling studies of the oceanic response to WWEs have shown that WWEs can force large surface and sub-surface temperature changes by modifying the zonal current structure in the central and eastern equatorial Pacific (Harrison and Giese 1988, Giese and Harrison 1990, 1991, Harrison and Craig 1993, Kindle and Phoebus 1995). It has also been

suggested that interaction between the WWE forced eastward propagating current pulse and the tropical instability wave (TIW) field in the central and eastern tropical Pacific can lead to enhanced waveguide warming (Harrison and Giese 1988, Giese and Harrison 1990, 1991). In modeling studies the background state of the model oceans can greatly influence the response to anomalous forcing (Schopf and Harrison 1983, Harrison and Schopf 1984, Harrison and Giese 1990); it is important to consider the background state of the ocean when determining the effect of anomalous forcing.

Case studies have found large amplitude local and remote changes to the oceanic temperature, current and sea surface height fields, related to the WWEs. Local response to WWEs involves surface cooling and freshening, a deepening of the mixed layer and strengthening of the thermocline, along with an eastward surface and westward subsurface current jet (McPhaden et al. 1988, McPhaden et al. 1992, Delcroix et al. 1993, Eldin et al. 1994, Smyth et al. 1996.a-b, Cronin and McPhaden 1997, Ralph et al. 1997, Feng et al. 1998). Remote changes observed to follow WWEs include eastward propagating increase in sea surface height, eastward surface current, net eastward equatorial transport, deepening of the thermocline, an increase in SST and upper ocean heat content (Eriksen et al. 1983, McPhaden et al. 1988, Kessler and McPhaden 1995, McPhaden 1999). There has been an indication of a relation between eastern Pacific biological productivity and Kelvin pulses related the westerly wind variability (Chavez et al. 1998). Analysis of the recent 1997-8 El Niño event has suggested that the genesis of the event can be traced to a series of periods of westerly wind in the western and central Pacific (Yu and Rienecker 1998, McPhaden, 1999). Strong westerly wind variability has occurred without leading to El Niño warming: one of the strongest periods of WWE activity in 1986-1998 occurred during the TOGA/COARE IOP in January 1993 (HV97); in spring 1993 eastern equatorial SSTA increased and briefly produced strong anomalies but SSTA then returned to normal and remained so for the rest of the year (see Fig. III.1.a). According to the BEI index of Harrison and Larkin (1998),

1993 was not an El Niño year.

Some statistical relationships between equatorial westerly wind variability and SSTA changes across the tropical Pacific were examined to help assess the theoretical, modeling and anecdotal evidence for a relationship between westerly wind variability and SSTA changes. The analysis was performed separately for periods in which the eastern tropical Pacific SSTA was initially close to normal and when it was warmer than normal. The WWE associated SSTA variability was compared with the SSTA variability when no equatorial WWEs occurred, to determine which features were associated with the WWEs and which showed no special relation to WWEs. This has been the first systematic statistical analysis to suggest that WWEs are a fundamental mechanism in the onset and maintenance of El Niño.

In the following sections I summarize the methods and results, and discuss some of the implications of the results. Section III.2 describes the datasets used and the statistical analysis method. The results of compositing SSTA for each WWE type are described in Section III.3. Section III.4 offers a summary and discussion of the main results.

### **III.2. Datasets and Methods**

The European Centre for Medium Range Weather Forecasts (ECMWF) 12-hourly  $2.5^{\circ}\times 2.5^{\circ}$  gridded 10-meter wind operational analysis (European Centre for Medium Range Weather Forecasts 1989), and the method described in Chapter II were used to identify all the WWEs in the period 1986-1997. The SST analysis used the Reynolds/NCEP weekly  $1^{\circ}\times 1^{\circ}$  gridded SST product (Reynolds and Smith 1994). A monthly climatology of SST was generated using the weekly SST data from 1984 through 1996 (those years are chosen to exclude the very anomalous periods of 1982-3 and 1997-8); SSTA was computed from this monthly climatology. Note that the analysis was repeated using other SST climatologies, and none of the principal results were affected.

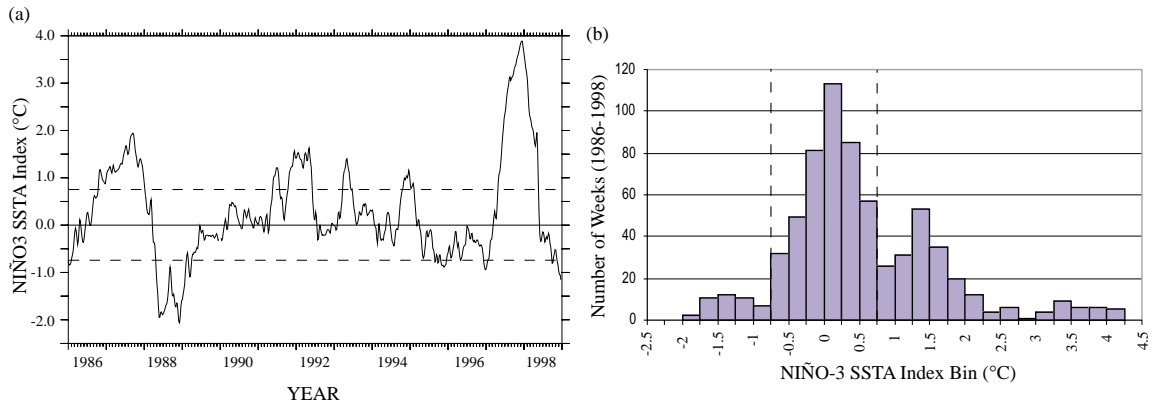


FIGURE III.1: (a) Weekly time-series of the NIÑO3 SSTA index used in this study, for the period 1986-1998. Dashed lines indicate the cutoffs for the three ENSO regimes (as defined in Section 2). Note how the El Niño events of 1986-88, 1991-92 and 1997-98, and the La Niña event of 1988-89 are identified by the index. (b) Histogram of the NIÑO3 SSTA index used in this study, for the period 1986-1998. The bin width is  $0.25^{\circ}\text{C}$ ; the dashed lines indicate the cutoffs for the three ENSO regimes (as defined in Section 2). Notice how there appear to be three distinct modes in this period.

To summarize the SSTA evolution following WWEs it is useful to consider separately events that occurred in different ocean/atmosphere states. Ideally, one would examine the evolution of the ocean in different periods of the seasonal cycle and in different phases of ENSO. Due to the limited data available (13 years), I only considered the different phases of ENSO separately. A widely used quantity to categorize the ENSO state of the ocean is the NIÑO3 SSTA index, defined as SSTA averaged over the region  $150^{\circ}\text{W}$ - $90^{\circ}\text{W}$ ,  $5^{\circ}\text{S}$ - $5^{\circ}\text{N}$ . Figure III.1 shows the time-series and histogram of the NIÑO3 index used here; the index identifies the El Niño events of 1986-8, 1991-2 and 1997-8 clearly, and the La Niña of 1988-9 is also evident. The distribution of NIÑO3 SSTA, shown in figure III.1.b, can be described as having three main states (cold, normal and warm), with a long tail on the warm side; this tail results from the large El Niño of 1997-8.

For the analysis, I describe the ocean as having 3 main states: COLD ( $\text{NIÑO3} < -0.75^{\circ}\text{C}$ ), REG ( $-0.75^{\circ}\text{C} < \text{NIÑO3} < 0.75^{\circ}\text{C}$ ), and WARM ( $\text{NIÑO3} > 0.75^{\circ}\text{C}$ ). Table III.1 shows the breakdown of WWEs by event type and NIÑO3 state 20 days before the WWE center day. Note that no equatorial WWEs occurred when the system was initially in a COLD state. Further discussion is limited to the REG and WARM states. The results de-

scribed in this paper are qualitatively unaffected by using thresholds between WARM and REG in the range  $0.25^{\circ}\text{C}$  to  $1.25^{\circ}\text{C}$ ; nor are they affected by ignoring the separation between COLD and REG states. Testing against a binomial distribution with probabilities determined by the total number of REG and WARM days, the Type C and E events have a distribution which shows a preference for the WARM periods, significant at the 99% level. This distribution is consistent with the interannual distribution of WWEs relative the Troup-SOI discussed in Chapter II, Section 6.a.

To examine the evolution of the SSTA field following the WWEs a series of composites were generated as in HV97. To quantify the composite SSTA evolution, I defined the SSTA change ( $\Delta\text{SSTA}$ ) relative to the WWEs as the difference between the SSTA at a given time and the SSTA 20 days before the center day of the WWE (Day (-20)). I generated both REG and WARM composites of SSTA and DSSTA for each WWE type from Day (-30) (30 days before center day) to Day (120) (120 days after center day). Since the distributions of the SSTA and DSSTA field are not normal, to test for statistical significance we use a bootstrap method (Efron and Tibshirani 1991), using 1000 bootstraps samples. The composite SSTA and  $\Delta\text{SSTA}$  fields are tested at the 95% level, for difference from a mean of zero.

TABLE III.1: Number of WWEs identified in the period 1986-1998, broken down by NIÑO3 SSTA condition 20 days before the WWE center day. The final row shows the percentage of all days which fall into each of the NIÑO3 SSTA condition bins. WWE types identified as in HV97, see Section 2 for a description of the NIÑO3 SSTA conditions. Bolding indicates the NIÑO3 SSTA state with a significant number of WWEs.

WWE Type	Total (1986-1998)	COLD (NIÑO3 < -0.75°C)	REGULAR (-0.75°C - NIÑO3 - 0.75°C)	WARM (NIÑO3 > 0.75°C)
W	41		<b>30</b>	11
C	72		39	<b>33</b>
E	56		19	<b>37</b>
Percentage of total days		11.0	60.6	28.4

To correctly interpret the relationship between SSTA variability and WWEs, it is necessary to understand how the evolution of SSTA following a WWE compares with the evolution of SSTA when there are no WWEs of that type. In order to interpret the SSTA/WWE associations, for each WWE type I constructed a series of WWE non-event composites, using a bootstrap method. First, all the dates that were not within 10 days of a center day for a particular WWE type were identified; those days were labeled as “non-event center days” for that particular WWE type. I then generated 1000 WARM and REG non-event SSTA and  $\Delta$ SSTA composites for each WWE type by randomly sampling (with replacement) the non-event center day list, the non-event composites go from Day (-30) through Day (120). At each location, for each composite day, the SSTA and  $\Delta$ SSTA non-event composite value was taken as the mean of the 1000 random non-event composites. Also computed were the percentage of non-event composites that had SSTA or  $\Delta$ SSTA values as large or larger than the corresponding event composite, which were used to compute the significance of the event composite relative to the non-event composite.

To explore the evolution of the SSTA field following periods when no WWEs of any of the three equatorial types occurred ALL/WARM and an ALL/REG non-event composites were generated, by excluding all equatorial WWE periods. The ALL non-event composites were computed from Day (-30) through Day (120) by using all days that were not within 10 days of any WWE center day as the non-event center days. The composites were computed using a bootstrap method (Efron and Tibshirani 1991), with 1000 bootstrap samples, and tested against a mean of zero at the 95% level.

### **III.3. Results**

Here I summarize the results from compositing SSTA and  $\Delta$ SSTA for each of the three equatorial WWE types, both for events and non-events (see Section III.2). Only those features in the composites that are significant at the 95% level are discussed. I first describe

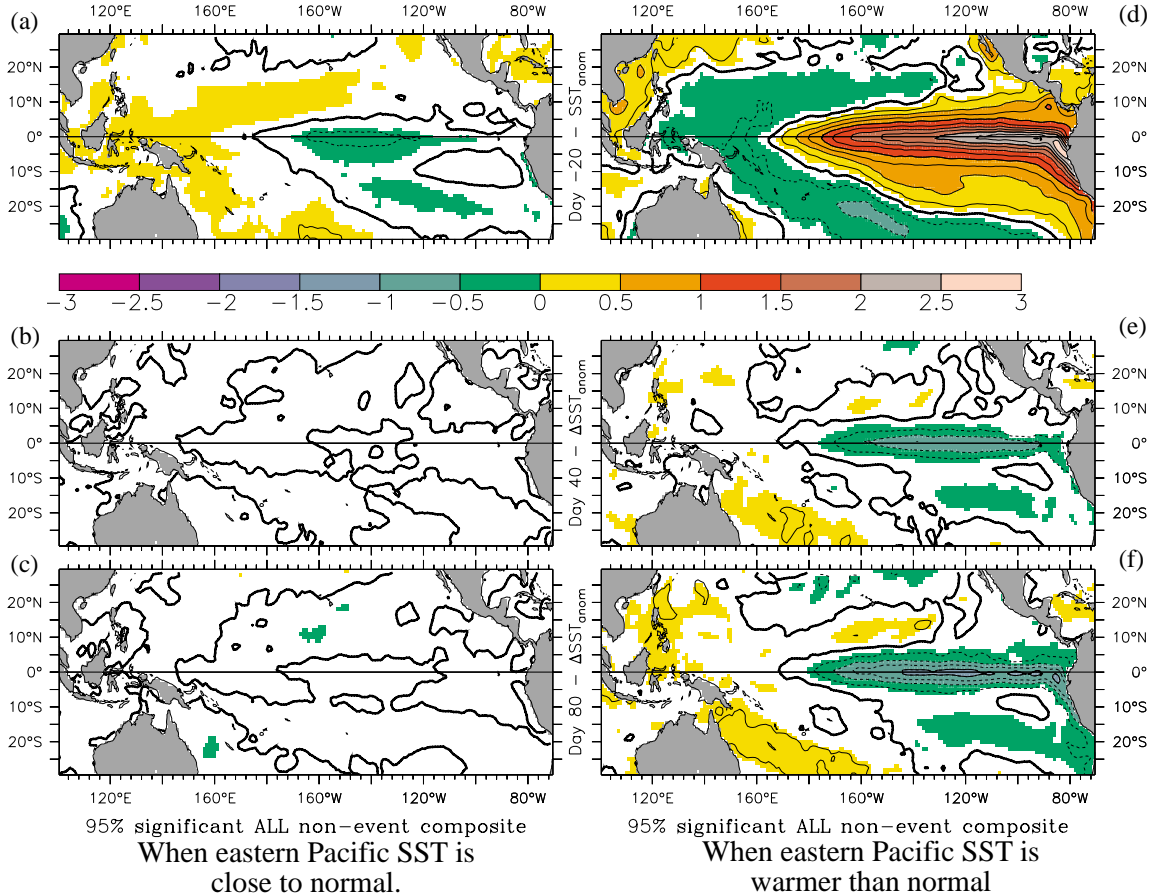


FIGURE III.2: ALL/REG non-event composite: (a) Day (-20) SSTA, and (b) Day (40), (c) Day (80)  $\Delta$ SSTA. ALL/WARM non-event composite: (d) Day (20) SSTA, and (e) Day (40), (f) Day (80)  $\Delta$ SSTA. Color shading indicates values which are significantly different (at the 95% level) from zero. Units are degrees centigrade, contour interval is 0.25°C, shading interval is 0.5°C.

the results of compositing SSTA and  $\Delta$ SSTA for non-WWE periods; these composites are viewed as the control experiments against which to compare the WWE event composites. The results of compositing for the three equatorial WWE types (W, C and E) are then described. The equatorial WWE event composites generally have SSTA changes significantly different (at the 95% level) from those in their respective non-event composites.

#### *a. Non-WWE Composites:*

The non-event composites for each individual WWE type had the same general characteristics. The individual/REG non-event composites are characterized by sparse areas of significance in the SSTA and DSSTA fields. Most individual/REG non-event com-

posites have only one significant SSTA feature; every individual/WARM non-event composites, on the other hand, has large regions of significant SSTA and a strong  $\Delta$ SSTA signal along the Pacific equatorial waveguide. Both the ALL/REG and ALL/WARM non-event composites have large-scale SSTA and  $\Delta$ SSTA patterns throughout the tropical Pacific, but the amplitude of the fields in the ALL/REG composite is much smaller than that of the ALL/WARM composite (Figure III.2). For both the ALL/WARM and individual/WARM non-event composites, the principal  $\Delta$ SSTA feature is cooling in the central and eastern Pacific equatorial waveguide.

The main feature for each of the individual/REG non-event composite Day (-20) SSTA field was weak warm ( $<0.25^{\circ}\text{C}$ ) values centered around  $10^{\circ}\text{N}$ , between  $160^{\circ}\text{E}$  and  $160^{\circ}\text{W}$ . The C/REG non-event composite also had weak cool ( $>-0.5^{\circ}\text{C}$ ) anomalies covering most of the NIÑO-3 region (see Figure III.4.b). None of the individual/REG non-event composites had any large-scale significant anomalies outside the Tropical Pacific basin. For none of individual/REG non-event composites were any  $\Delta$ SSTA fields significant (even at the 90% level).

Figure III.2.a-c shows the Day (-20) SSTA and the Day (40) and (80)  $\Delta$ SSTA field for the ALL/REG non-event composites, the features significant at the 95% level are highlighted by shading. The SSTA for the ALL/REG non-event composite tends to be close to normal across the basin, with slightly cooler than normal values in the central equatorial Pacific. When no WWEs occurred in the period 1986-1998, and NIÑO3 SSTA was initially close to zero, there was no tendency for eastern and central Pacific warming; none of the SSTA changes exceed  $0.25^{\circ}\text{C}$ . In the absence of WWEs and NIÑO3 SSTA was close to zero, tropical Pacific SST tended to remain near climatology.

The features of the individual/WARM non-event composite contrast sharply with the individual/REG non-event composite: the Day (-20) SSTA amplitudes are large, there are large-scale  $\Delta$ SSTA values in the tropical Pacific as well as SSTA features outside the

tropical Pacific region. The Day (−20) individual/WARM non-event composite SSTA field is dominated by El Niño type anomalies in the tropical Pacific, and weak warm ( $<0.5^{\circ}\text{C}$ ) anomalies in the Indian and northern tropical Atlantic Oceans. The tropical Pacific has strong ( $>1.5^{\circ}\text{C}$ ) composite anomalies between  $5^{\circ}\text{S}$  and  $5^{\circ}\text{N}$  east of the dateline, and along the northwest coast of South America. There are weak cold anomalies poleward and west of the warm El Niño anomalies. The individual/WARM non-event composite  $\Delta\text{SSTA}$  fields for the individual WWE types are confined to the tropical Pacific, and are dominated by moderate to strong cooling of the central and eastern equatorial waveguide. By Day (80), the waveguide cooling exceeds  $-0.75^{\circ}\text{C}$  in all the individual non-event composites. The composites also show weak cooling in the southeast Pacific, and weak warming in the southwest Pacific; the amplitude of these changes are all less than  $0.5^{\circ}\text{C}$ .

Figure III.2.d-f shows the ALL/WARM non-event composite Day (−20) SSTA, and the Day (40) and (80)  $\Delta\text{SSTA}$  fields, highlighting significant values by shading. The fields are all qualitatively similar to the individual/WARM non-event composites, however the amplitude of the changes is larger in the ALL/WARM non-event composite. In the Day (−20) SSTA field, the El Niño type features are apparent, with strong warm eastern and central equatorial Pacific anomalies, and weak cold anomalies poleward and west of these. The warm anomalies in the Indian and northern tropical Atlantic Oceans are present in the ALL/WARM non-event composite. The cooling of the central and eastern equatorial waveguide is pronounced in the Day (40) and (80)  $\Delta\text{SSTA}$  fields, as is the weak warming of the southwestern and cooling of the southeastern part of the basin. The changes by Day (40) are generally of the opposite sign as the anomalies on Day (−20). For the period 1986-1998, when NIÑO3 SSTA was initially warm and no WWEs occurred, the tropical Pacific tended to return towards climatological SST.

*b. Equatorial WWE Composites:*

I now examine the SSTA composites for each of the three equatorial WWE types

(W, C and E). The composite SSTA evolution for each of the equatorial WWE composites are shown in Figures III.3, III.5 and III.6; the panels on the left (right) half of each figure show the evolution of the REG (WARM) composite. Color shading indicates statistically significant SSTA or  $\Delta$ SSTA values. The contour interval is  $0.25^{\circ}\text{C}$ , positive (negative) values are indicated warm (cold) colors, and the dark contour indicates the zero line. The upper panels (Fig. III.3.a, III.3.g) show composite SSTA on Day (-20). The lower panels (Fig. III.3.b-3.f, III.3.h-3.l) show the evolution of the  $\Delta$ SSTA in 20 day increments, from the center day (Fig. III.3.b) to Day (+80) (Fig. III.3.f). For reference, in all the panels the WWE classifying region is indicated by a blue box.

i) W/REG COMPOSITE

The composite initial SSTA structure for the W/REG event composite (Fig. III.3.a) exhibits weak cold anomalies in the southeast tropical Pacific, weak warm anomalies extending to the northeast from the central equatorial Pacific and cold anomalies poleward and westward of the warm anomalies. None of the anomalies exceed  $0.75^{\circ}\text{C}$  in the composite. Compared to the W/REG non-event composite, the W/REG event composite SSTA field on Day (-20) is warmer in the region  $160^{\circ}\text{E} - 120^{\circ}\text{W}$ ,  $5^{\circ}\text{S} - 5^{\circ}\text{N}$  by  $0.5^{\circ}\text{C}$ , and cooler poleward and west of the warm waveguide deviations from the W/REG non-event composite. Outside the Pacific basin there are also anomalies and deviations from the non-event anomalies. The eastern Indian ocean south of Indonesia is cool; and the anomaly is cooler than that of the W/REG non-event composite by  $-0.25^{\circ}\text{C}$ . There is also a broad region of weakly cold water (cooler than the non-event composite as well) covering the southern hemisphere tropical Atlantic Ocean. Both extra-Pacific Day (-20) SSTA patterns appear when the anomalies are masked at the 99% level.

The composite  $\Delta$ SSTA structure is characterized by cooling in the W region, warming along the equatorial waveguide and the northwest coast of South America, and warming in the southeastern Pacific (Fig. III.3.b-III.3.f). The cooling under the main WWE appears

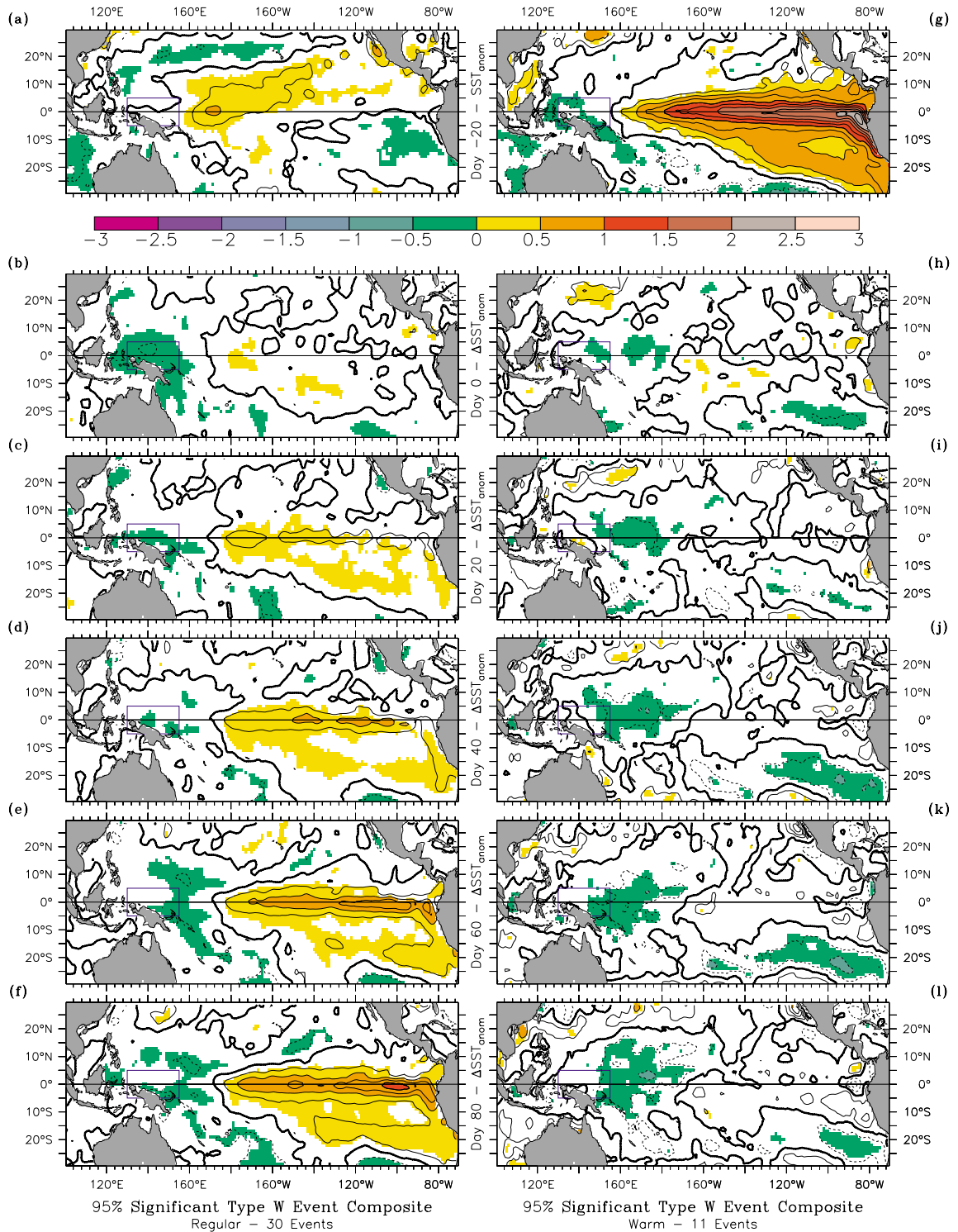


FIGURE III.3: W/REG event composite: (a) Day (-20) SSTA, and (b) center day, (c) Day (20), (d) Day (40), (e) Day (60), (f) Day (80)  $\Delta$ SSTA. W/WARM event composite (g) Day (-20) SSTA, and (h) center day, (i) Day (20), (j) Day (40), (k) Day (60), (l) Day (80)  $\Delta$ SSTA. Values significantly different than zero at the 95% level are highlighted by color shading. Units are degrees centigrade, contour interval is 0.25°C, shading interval is 0.5°C. The classifying region is indicated by the purple box in each figure.

during the lifetime of the WWE and remains through Day (80); the cooling is less than  $0.5^{\circ}\text{C}$ . The equatorial waveguide warming is apparent by Day (20), and it expands and increases in amplitude through Day (80). The main warming is contained between  $130^{\circ}\text{W}$  and the South American coast, and exceeds  $0.75^{\circ}\text{C}$  by Day (80); the warming leads to warm anomalies along the equatorial waveguide and the South American coast by Day (60). There is no conspicuous propagation to the  $\Delta\text{SSTA}$  pattern, rather a general spreading and amplification. The warming in the southeast Pacific happens by Day (20) and expands through the compositing period, the amplitude is between  $0.25^{\circ}\text{C}$  and  $0.5^{\circ}\text{C}$ . There is a minimum in composite  $\Delta\text{SSTA}$  amplitude between the waveguide warming and the southeast Pacific warming. The cooling in the classifying region, the waveguide warming and the southeast Pacific warming are all different from the changes in the W/REG non-event composite.

#### ii) W/WARM COMPOSITE

The SSTA structure in Day (-20) of the W/WARM composite event is similar to that seen in the ONSET and PEAK phases of ENSO (Rasmusson and Carpenter 1982, Harrison and Larkin 1998). There is warm SSTA east of  $160^{\circ}\text{E}$ , along the northwest coast of South America and in the southeastern Pacific (Fig. III.3.g). There are weak cold anomalies in the eastern Indian Ocean and the western Pacific Ocean. The cold anomalies do not exceed  $0.25^{\circ}\text{C}$ , while the equatorial warm anomalies exceed  $1.0^{\circ}\text{C}$  east of the dateline. There is an area of minimum in the SSTA amplitude in the southeast Pacific between the warm coastal and waveguide anomalies, and the southeast Pacific Ocean anomalies. The W/WARM event SSTA field in the tropical Pacific basin is not different from the non-event SSTA field on Day (-20), except for slightly warmer anomalies between  $150^{\circ}\text{E}$  and the dateline, and  $5^{\circ}\text{S}$  and  $5^{\circ}\text{N}$ . On Day (-20) there are deviations from the W/WARM non-event composite outside the Pacific basin: the warm Indian Ocean anomalies are smaller and actually become negative close to the maritime continent, and there are moderate ( $>0.5^{\circ}\text{C}$ ) cool anomalies in the Gulf of Guinea in the Atlantic Ocean.

Following the W/WARM WWE, there is very little structured  $\Delta$ SSTA, the main feature being cooling in the W region (Fig. III.3.h-3.1). The cooling under the main wind anomalies is between  $0.25^{\circ}\text{C}$  and  $0.5^{\circ}\text{C}$  and persists through Day (80). There is weak cooling in the southeast Pacific by the center day, which disappears by Day (20). There is some warming near the Equator in the central Pacific, but it is not persistent nor does it exceed  $0.25^{\circ}\text{C}$ . The SSTA changes in the W/WARM event composite are seen to be primarily local to the wind event region. When compared with the W/WARM non-event composite, an interesting pattern emerges. While the waveguide  $\Delta$ SSTA values in the composite are not significantly different from zero, compared with the non-event composite there is large amplitude reduced cooling. By Day (80), the waveguide DSSTA values in the event composite exceed those in the non-event composite by over  $0.5^{\circ}\text{C}$  from the dateline to the coast of South America. The cooling in the Type W classifying region is significantly larger than that which appears in the non-event composite.

### iii) C/REG COMPOSITE

The Day (-20) composite SSTA field for the C/REG composite shows some large-scale extra-tropical SSTA features similar to those in the W/REG composite. I show the Day (-20) SSTA field for the C/REG event, non-event and the difference (event minus non-event) in Figure III.4.a-c to illustrate the features. The large-scale central Pacific warm anomalies, and the western Pacific, eastern Indian and southern hemisphere Atlantic cold SSTA is evident in figure III.4.a. It is clear from figures III.4.b and III.4.c that these features are quite different from those in the C/REG non-event composite. Figure III.5.a focuses on the Day (-20) tropical Pacific SSTA features of the C/REG event composite. The band of warm water extending to the northeast of the warm water core just east of the classifying region is clear, as is the cool water poleward and west of it.

The event  $\Delta$ SSTA composite shows three main patterns: cooling under the main WWE wind anomalies, warming along the equatorial waveguide and the northwest coast of

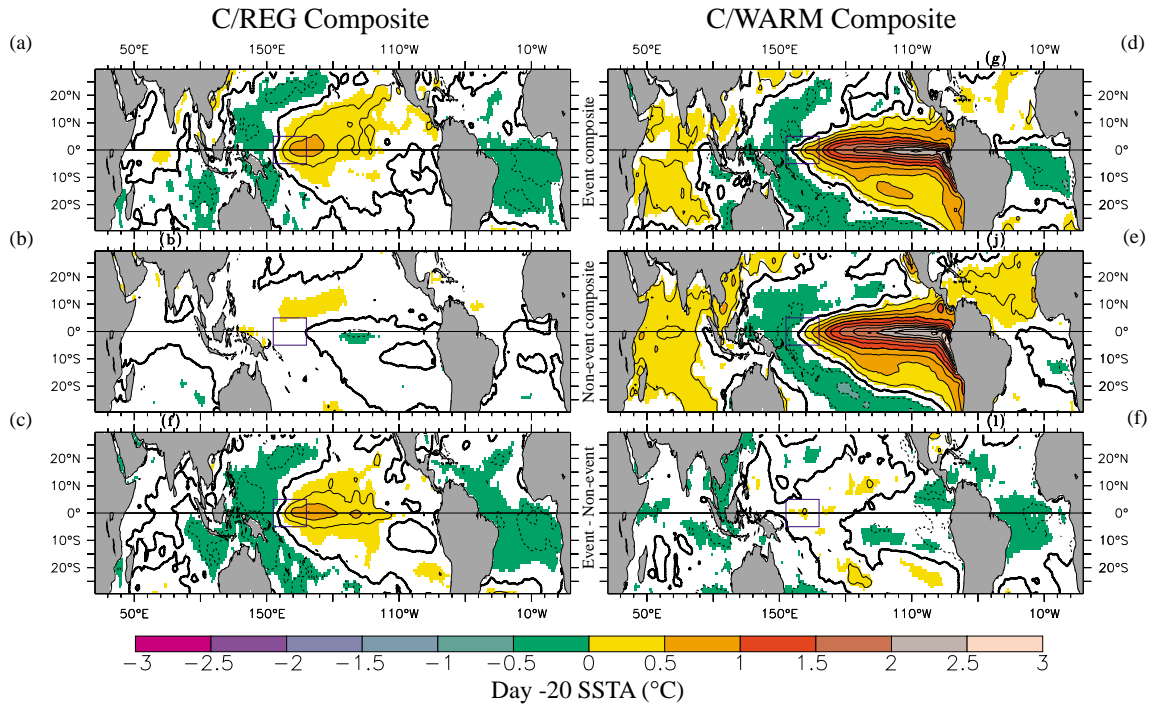


FIGURE III.4: C/REG Day (-20) SSTA for the (a) event composite and (b) non-event composite, and (c) difference between the Day (-20) event composite SSTA and the Day (-20) non-event composite SSTA. C/WARM Day (-20) SSTA for the (d) event composite and (e) non-event composite, and (f) difference between the Day (-20) event composite SSTA and the Day (-20) non-event composite SSTA. Units are degrees centigrade, contour interval is  $0.25^{\circ}\text{C}$ , shading interval is  $0.5^{\circ}\text{C}$ . The classifying region is indicated by the purple box in each figure

South America, and warming in the southeast Pacific (Fig. III.5.b-III.5.f). The cooling under the event happens during the period of maximum westerly anomalies and exceeds  $0.25^{\circ}\text{C}$ . The warming in the southeast Pacific happens by Day (20) and remains through Day (80). The equatorial waveguide and South American coastal warming is evident on Day (40), and remains through Day (80) intensifying and expanding with time. The warming exceeds  $0.5^{\circ}\text{C}$  east of  $160^{\circ}\text{W}$  by Day (80), and close to the northwest coast of South America it exceeds  $1.0^{\circ}\text{C}$ . The warming along the waveguide and the coast of South America leads to warm anomalies by Day (60) east of  $120^{\circ}\text{W}$ . The waveguide and South American coast warming exceeds that in the non-event composite by over  $0.5^{\circ}\text{C}$  by Day (80), the southeast Pacific warming exceeds that in the non-event composite by  $0.25^{\circ}\text{C}$  from Day (20) on, and the cooling under the WWE is significantly different from the non-event composite changes.

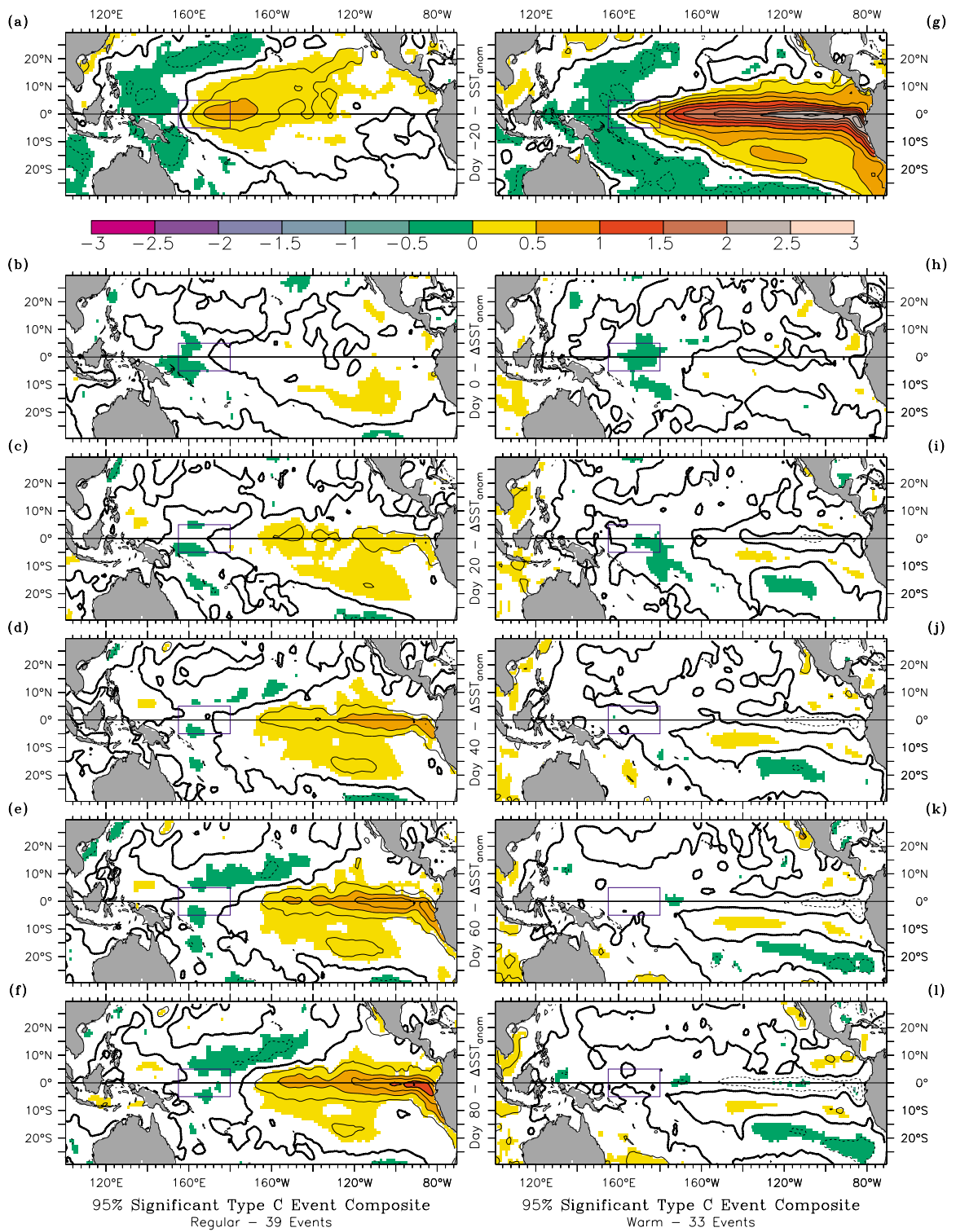


FIGURE III.5: As in Figure III.3, except for the C/REG (a)-(f) and C/WARM (g)-(l) event composites.

## iv) C/WARM COMPOSITE

The Day (-20) SSTA field across all tropical oceans for the C/WARM event, non-event and difference (event minus non-event) is shown in Figure III.4.d-f. Figure III.5.g shows the Day (-20) C/WARM event composite SSTA field in the tropical Pacific. The initial tropical Pacific SSTA structure for the C/WARM event composite is qualitatively similar to the type C/WARM non-event composite, but there are areas of small amplitude differences between the two. On Day (-20) the composite SSTA exceeds  $1.0^{\circ}\text{C}$  east of  $170^{\circ}\text{W}$  along the equator to the northwest coast of South America. The C/WARM event composite SSTA on Day -20 is significantly cooler than the non-event composite along the northwest coast of South America and in the South China Sea – the differences are all less than  $0.5^{\circ}\text{C}$ . Extra-Pacific SSTA patterns, similar to those which appear in the W/WARM event composite are evident in Figure III.4: the SSTA in the Gulf of Guinea and in the eastern Indian Ocean are both weakly cooler than zero and than the C/WARM non-event composite.

The  $\Delta\text{SSTA}$  event composite (Fig. III.5.h-III.5.l) has almost no large-scale features, and the amplitude of the changes is generally less than  $0.25^{\circ}\text{C}$ . The main cooling pattern is underneath the main WWE surface wind anomalies; it occurs during the period of maximum westerly anomalies, and disappears by Day (40). There is weak warming south of the equatorial waveguide beginning Day (20), remaining there through Day (80). There is a patch of warm water off the west coast of Mexico, which appears in Day (60). Even though there are no equatorial waveguide changes in the C/WARM event composite, the  $\Delta\text{SSTA}$  values are different from those of the C/WARM non-event composite. Relative to the non-event composite, the C/WARM composite is characterized by reduced waveguide cooling that extends from the dateline to the coast of South America by Day (60), and exceeds  $0.5^{\circ}\text{C}$  east of  $140^{\circ}\text{W}$ .

## v) E/REG COMPOSITE:

The E/REG composite has an initial structure (Fig III.6.a) similar to the W/REG and C/REG event composites. On Day (-20) the western Pacific is cooler than in the E/REG non-event composite (by more than  $0.25^{\circ}\text{C}$ ) and the central equatorial Pacific is warmer than in the non-event composite by over  $0.25^{\circ}\text{C}$  from  $160^{\circ}\text{E}$ - $120^{\circ}\text{W}$ . There are also weak extra-Pacific SSTA features which are less than zero and than the E/REG non-event composite. The tropical Atlantic Day (-20) SSTA is less than zero (SSTA exceeds  $-0.5^{\circ}\text{C}$  in Gulf of Guinea) and than the non-event composite; the SSTA in the eastern Indian Ocean is less than  $-0.25^{\circ}\text{C}$ , and is cooler than the non-event composite SSTA. Both extra-Pacific features are significant at the 99% level.

The  $\Delta\text{SSTA}$  composite (Fig. III.6.b-III.6.f) exhibits an evolution similar to that seen in the C/REG and W/REG composites, except the SSTA changes under the WWE are warming rather than cooling. There is warming in the classifying region, occurring during the lifetime of the WWE, the warming remains through the compositing period and by Day (20) exceeds  $0.5^{\circ}\text{C}$ . There is warming in the southeast Pacific, appearing by the center day, and intensifying following Day (60). The equatorial waveguide warms following the event, the warming slowly spreads east. There is some warming in the western Pacific, peaking near Day (80) at  $0.25^{\circ}\text{C}$ . The waveguide, southeast Pacific and western Pacific warming are all greater in the event composite than in the non-event composite.

## vi) E/WARM COMPOSITE:

None of the SSTA or  $\Delta\text{SSTA}$  patterns for the E/WARM composite are different from the E/WARM non-event composite. The initial SSTA structure (Fig. III.6.g) shows the same El Niño anomalies that were seen in all previous WARM composites. The main feature of the  $\Delta\text{SSTA}$  field (Fig. III.6.h-III.6.l) is cooling along the eastern and central equatorial waveguide, which exceeds  $-0.5^{\circ}\text{C}$  by Day (60). There is also weak warming in the eastern Indian Ocean. The cooling in the central Pacific basin, while not distinguishable

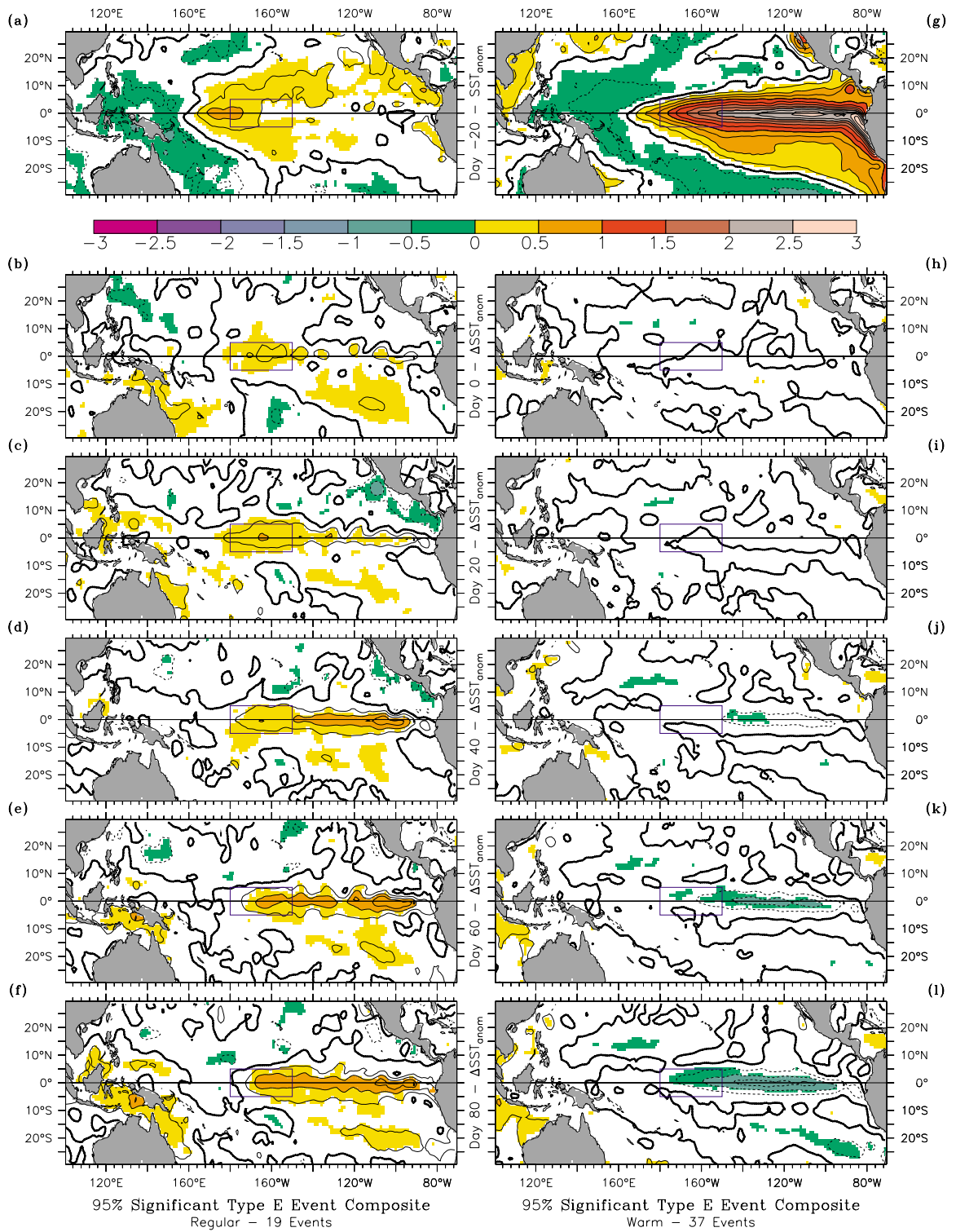


FIGURE III.6: As in Figure III.3, except for the E/REG (a)-(f) and E/WARM (g)-(l) event composites.

from that which is seen in the E/WARM non-event composite, is of smaller amplitude than that of the ALL/WARM non-event composite.

#### **III.4. Summary and Discussion**

Using the WWE classification scheme of HV97 and the Reynolds/NCEP weekly global SST analysis (Reynolds and Smith 1994), I have composited the SSTA changes following the three equatorial types of WWEs (W, C and E), between 1986 and 1998. These changes were compared with those occurring in the absence of WWEs. The focus is on the tropical Pacific because of our interest in the role(s) of equatorial WWEs in the onset and maintenance of ENSO warm SSTA. I argue that WWEs are a fundamental part of the appearance of warm conditions in the central and eastern equatorial Pacific, and for the maintenance of warm conditions during El Niño events.

In this section I summarize the results of our compositing analysis, and discuss the relation of these results to previous theoretical, modeling and observational studies. I first summarize the SSTA evolution in the absence of equatorial WWEs, followed by a summary of the local and remote SSTA evolution following different types of WWEs, and conclude by connecting these results to the dynamical mechanisms proposed for WWE/ocean interaction.

##### *a. SSTA Evolution in the Absence of WWEs:*

In the absence of equatorial WWEs, the tropical Pacific ocean SST field tended to remain at or return toward climatological values (Section III.3.a). When NIÑO3 SST is initially close to climatology, tropical Pacific SST remains near climatology (see Fig. III.2.b-c). When the NIÑO3 SSTA was initially warmer than normal, there was moderate to strong cooling (as much as  $-1.0^{\circ}\text{C}$  in the composite) of the central and eastern equatorial Pacific waveguide surface waters. This cooling tended to reduce the pre-existing warm El Niño type anomalies (see Fig. III.2.e-f).

*b. Local SSTA Changes following WWEs:*

By local SSTA changes I mean those which occur under the composite WWE wind anomalies, both inside the WWE identification region and adjacent to it. The second and third columns of Table III.2 summarize the character of the local SSTA changes following each of the WWE types and their departures from the non-event composite. Local changes that were significantly different from zero were also significantly different from the non-event composites.

The Type W and C WWEs exhibited local SSTA cooling during the lifetime of the WWE. The composite cooling was generally less than  $0.25^{\circ}\text{C}$ , and everywhere less than  $0.5^{\circ}\text{C}$ ; the cooling occurred irrespective of the initial eastern Pacific SSTA (see Figs. III.3,.5). Although small, this cooling was a significant feature of the composites at the 99% confidence level.

The Type E WWEs have a different local SSTA change than that of the western equatorial WWEs. Following Type E events, when NIÑO3 SST is initially close to climatology, there is SSTA warming in the WWE defining region (see Fig. III.6). When NIÑO3

TABLE 2: Summary of the principal  $\Delta\text{SSTA}$  values and departures from the non-event composites for each of the equatorial WWE types, for both REG and WARM event composites. Plus signs (+) indicate that the  $\Delta\text{SSTA}$  value or departure from the non-event composite was significantly greater than zero. Minus signs (-) indicate that the SSTA change or departure from the non-event composite was significantly less than zero. Double plusses (++) indicates that the dominant changes or departures had an amplitude greater than  $0.5^{\circ}\text{C}$ .

NIÑO-3 SSTA	Event Type	Local		Central and Eastern Pacific Waveguide		SE Tropical Pacific	
		Value	Departure	Value	Departure	Value	Departure
REGULAR ( $-0.75^{\circ}\text{C}$ - and $\square 0.75^{\circ}\text{C}$ )	<i>W</i>	-	-	++	++	+	+
	<i>C</i>	-	-	++	++	+	+
	<i>E</i>	+	+	++	++	+	+
WARM ( $>0.75^{\circ}\text{C}$ )	<i>W</i>	-	-		++	-	
	<i>C</i>	-	-		++	-	
	<i>E</i>		+	-		-	

was warmer than normal there were no local SSTA changes; however the E/WARM event SSTA change composite exhibits less cooling than is seen in the E/WARM the non-event composite.

*c. Remote SSTA Changes following WWEs:*

The period following some WWE types exhibited large-scale SSTA changes and departures from the evolution of the non-event composites far from the main WWE wind anomalies; these also are summarized in Table III.2. The remote SSTA changes depended on the initial NIÑO3 SSTA. Generally the central and eastern Pacific equatorial SSTA field warmed or remained warm.

When the NIÑO3 SST was initially close to climatology, the WWEs centered on the equator were followed by large-scale remote SSTA changes. The main features were: warming of the central and eastern equatorial Pacific along the equatorial waveguide and the north-west coast of South America; cooling in the western Pacific; and warming in the southeastern Pacific (see Figs. III.3,.5,.6). The composite waveguide warming following the Type W and C WWEs exceeded 1.0°C 80 days after the event, while the western Pacific cooling and southeast Pacific warming was of small amplitude (0.25-0.5°C). The amplitude of these SSTA changes is of the same general structure as that seen in the onset of El Niño, and the amplitudes are large enough to account for a large part of the observed composite El Niño warming (see Rasmusson and Carpenter 1982, Harrison and Larkin 1998).

There is no waveguide warming associated with the WARM event composites for any equatorial WWE type; nonetheless these represent significant departures from the non-event composites (since the expected change in the absence of a WWE is for waveguide cooling). The W/WARM and C/WARM event composites had no cooling of central and eastern waveguide SSTA, which when compared with the non-event composite amounted to maintenance of the warm waveguide SSTA values (recall that the departures from the non-event composite exceeded 0.5°C). The timing of these departures is similar to the changes

and departures seen in the W/REG and C/REG composites; however the departures are much more pronounced in the central equatorial Pacific than in the eastern Pacific. Also, the maximum amplitude of the deviations from the non-event composite in these two equatorial WARM composites is only 66% of the maximum deviation in the respective REG event composites.

*d. Discussion:*

The local cooling seen in the Type C and W event composites is in agreement with the available case studies of the evolution of local SST following WWEs in the western Pacific warm pool (McPhaden et al. 1988, McPhaden et al. 1992, Delcroix et al. 1993, Eldin et al. 1994, Smyth et al. 1996, Cronin and McPhaden 1997, Feng et al. 1998). The range of the amplitude of the observed local cooling under individual WWEs has been 0.2°C-0.6°C over the period of a week (McPhaden et al. 1988, McPhaden et al. 1992, Delcroix et al. 1993, Eldin et al. 1994); recall the composite amplitudes were between 0.25°C and 0.5°C. Observations of SST evolution under a series of WWEs which quickly follow each other has shown larger cooling, between 0.8°C and 1.0°C, over a period of a few weeks (Smyth et al. 1996.b, Cronin and McPhaden 1997); unsurprisingly, a sequence of WWEs in succession impact the local ocean more strongly than individual WWEs. The agreement between the various observations of local SST changes following individual WWEs, and with the composite behavior over 13 years, suggests that the local changes observed in the case studies were representative of the local SST evolution following WWEs.

There have been many mechanisms suggested for local SST cooling under strong winds in the western equatorial Pacific. During the TOGA/COARE Intensive Observational Period, the evolution of the western equatorial Pacific during a series of WWEs was observed more thoroughly than ever before; this allowed exploration of the factors controlling SST variability during the observed WWE periods. In a 1-D analysis of the heat balance at (156°E, 0°), Cronin and McPhaden (1997) argue that the local warm pool SST

variability under WWE conditions was controlled by decreased incoming short-wave radiation and increased latent heat-flux; they note that zonal advection also plays an important role. Feng et al. (1998) did a 3-D heat and salinity budget in the western Pacific during the same period, centered at (156°E, 2°S); and found that both zonal and meridional advection of heat and salt played an important role in the budgets under WWE conditions, and acted both to increase the surface salinity and to reduce surface temperature. According to Feng et al. (1998), cooling through meridional advection dominated warming due to zonal advection during the January 1993 western Pacific WWE. Evidently there remains some uncertainty about the processes responsible for local cooling under Type C and W WWEs; no single process is expected to apply to every event.

I am not aware of any case studies of the local response to Type E WWEs. I suggest that the character of the local SSTA evolution following a Type E WWE is due to the Type E classifying region being dominated by strong and persistent trade winds. These trade winds lead to equatorial upwelling through Ekman divergence at the surface, as well as to a generally strong westward surface current. Climatologically, both the upwelling and the westward current act to cool the local SST by advection of cooler waters (the zonal temperature gradient is generally negative, except during the most extreme of El Niño events). Westerly anomalies in this region would lead to reduced Ekman divergence and upwelling, and reduced westward surface current; both of which would contribute to warm the surface waters. The latent surface fluxes of heat would be reduced since the WWEs, in all but the most extreme cases, result in reduction of the wind speed (HV97). Reductions in easterly trade winds should be expected to lead to local SST warming, as is seen in the Type E composite.

Only one case study of the remote changes in SST following WWEs is known to me: McPhaden *et al.* (1988) describe an eastward propagating current pulse generated by a western Pacific WWE during May 1986. This pulse was associated with warming of 1°C at

(110°W,0°N) in mid-June 1986 (30 days after the WWE); according to McPhaden *et al.* (1988) the warming pulse following the WWE had little effect on the evolution of the subsequent 1986-7 El Niño event. Harrison and Giese (1989) offer a different interpretation of the same event; they agree that the June-1986 warming at 110°W is the result of the first baroclinic mode Kelvin pulse excited by the May WWE, and is short lived. However, using current data from moorings on the Equator at 140°W and 110°W, they argue that a second phase of warming occurring in mid-July 1986 was the result of the second baroclinic mode Kelvin pulse forced by the WWE; this pulse was related to SST warming of over 2.0°C at the onset of the 1986-7 El Niño. Both McPhaden *et al.* (1988) and Harrison and Giese (1989) argue that zonal and meridional advection of heat played an important role in the eastern Pacific SST warming forced by the WWE.

Though WWEs have been suggested as an important mechanism in the evolution of ENSO, there have been no other observational attempts at describing the remote SST changes following WWEs. Some observational studies have found eastern and central Pacific thermocline (as defined by the depth of the 20°C isotherm) and sea surface height changes following WWEs, and have suggested a relationship between ENSO warming and WWEs (Eriksen *et al.* 1983, Hayes *et al.* 1991, Kessler and McPhaden 1995, Chavez *et al.* 1998, Yu and Rienecker 1998, McPhaden 1999). This present study is the first to systematically describe the remote SSTA changes that occur following equatorial WWEs.

The composite remote SSTA changes reported here when NIÑO3 SST is close to climatology are consistent with the results from ocean general circulation model (OGCM) experiments described in the literature. Examining the response of the OGCM to idealized WWE forcing, Harrison and Giese (1988), and Giese and Harrison (1990, 1991) found that WWEs drove warming in the eastern and central equatorial Pacific in excess of 0.5°C; the warming appeared at 140°W within a month of the anomalous forcing and continued for over three months. The SST warming in the OGCM was driven primarily by zonal advective

tion by equatorially trapped eastward propagating current pulses, and by meridional advection due to interaction of these pulses with the background tropical instability wave (TIW) field. Note that the WWE forcing used in those model experiments had an estimated zonal extent of  $10^\circ$  longitude, which is about  $1/3$  the average zonal extent of WWEs; the response to a WWE of larger zonal extent would be more than that described in the mentioned experiments. The large amplitude composite response relative to the OGCM experiments ( $1.0^\circ\text{C}$  vs.  $0.5^\circ\text{C}$ ) could be the result of the underestimation of the WWE zonal extent by Harrison and Giese (1988), and Giese and Harrison (1990,1991) or due to some ocean/atmosphere coupling which would be absent in their model; the timing and structure of the SSTA composite changes when NIÑO3 SST is initially close to climatology are consistent with those of the OGCM experiments. Chapter V further explores the ability of the model to reproduce the composite SSTA changes.

The composite remote changes to the SSTA fields when NIÑO3 SST is initially warmer than climatology, for the Type W and C events, is not like that described in the literature. The sensitivity of the SSTA associations with WWEs to initial state of the ocean/atmosphere is not unexpected. Schopf and Harrison (1983) and Harrison and Schopf (1984) found that the eastern Pacific temperature response following a period of westerly wind anomaly was larger when the forcing was in the northern winter months than in the northern summer months. The difference in response in the two cases was due the equatorial zonal temperature gradients and the TIW activity being much stronger in boreal winter than in boreal spring. The difference in amplitude of the maximum departures from non-event SSTA changes between the WARM and REG events could be similarly explained.

The warming associated with El Niño leads to a reduced magnitude of the equatorial zonal temperature gradients; in extreme cases such as the peak of the 1997-8 El Niño the zonal temperature gradient disappears or even reverses. For the period 1986-1998, when the NIÑO3 SSTA index was close to normal (within  $0.75^\circ\text{C}$  of climatology) the mean zonal

SST gradient on the equator was:  $-7.0 \times 10^{-7} \text{ }^\circ\text{C/m}$  at  $170^\circ\text{W}$ ,  $-5.5 \times 10^{-7} \text{ }^\circ\text{C/m}$  at  $140^\circ\text{W}$ , and  $-5.7 \times 10^{-7} \text{ }^\circ\text{C/m}$  at  $110^\circ\text{W}$ ; but for periods where the NIÑO3 SSTA index exceeded  $0.75^\circ\text{C}$ , the equatorial zonal temperature gradient was:  $-1.6 \times 10^{-7} \text{ }^\circ\text{C/m}$  at  $170^\circ\text{W}$ ,  $-5.3 \times 10^{-7} \text{ }^\circ\text{C/m}$  at  $140^\circ\text{W}$ , and  $-4.0 \times 10^{-7} \text{ }^\circ\text{C/m}$  at  $110^\circ\text{W}$ . Even though the magnitude is reduced in warm NIÑO3 periods, the average zonal SST gradient across the equator is negative both in periods of near normal and warm NIÑO3 SST. If the current response following the WWE were comparable when the NIÑO3 SST is close to and warmer than climatology, the temperature response due to zonal temperature advection when NIÑO3 was initially warm would be smaller.

It has been suggested that that an important mechanism leading to eastern equatorial Pacific SST warming following a WWE, is anomalous meridional advection of heat due to interaction between the WWE forced Kelvin pulse and the tropical instability waves (Harrison and Giese 1988, Giese and Harrison 1990, 1991). In the absence of TIWs that process would not be able to increase the equatorward surface heat flux, and the SST response would be smaller than in the presence of TIWs. Decreased TIW activity during El Niño is a possible contributing factor to the decrease in eastern Pacific SSTA changes to following WWEs in initially warm NIÑO3 conditions.

This compositing study describes the average SSTA changes that follow the various WWE types, however the SSTA changes following any individual WWE may be different from the composite. Figure III.7 shows scatter plots of the NIÑO3 SSTA on Day (-20) vs. the NIÑO3 DSSTA on Day (60) for the equatorial WWE types and for non-event periods, the horizontal lines show the composite values for both eastern Pacific SSTA regimes. Figure III.7 highlights those WWEs of strong intensity by using red marks on the plots; we define strong events to be those events whose wind measure statistic exceeds  $1.5 \times 10^6 \text{ m}$  (wind measure is a time integral of the spatially averaged zonal wind anomaly of each WWE; see Chapter II, HV97). It is apparent in these scatter plots that the changes to eastern

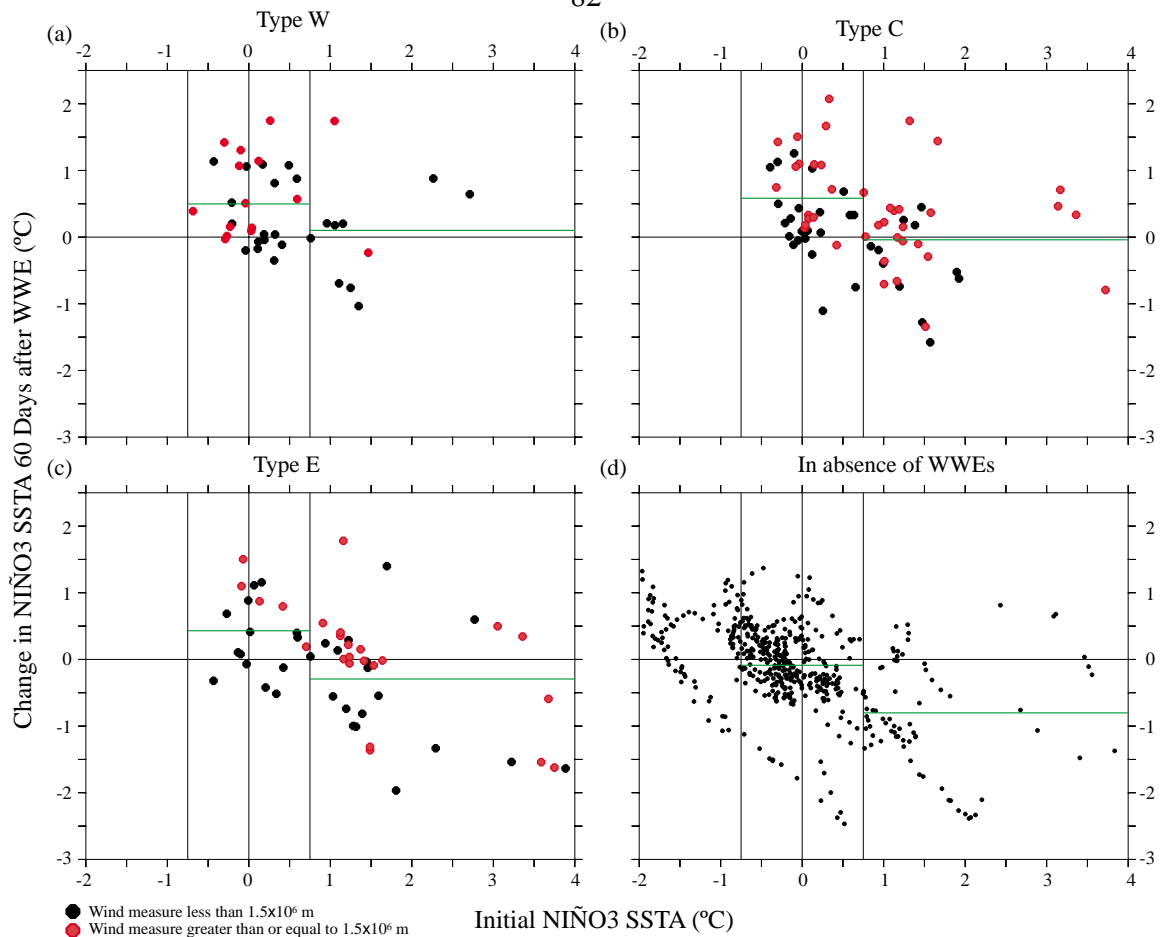


FIGURE III.7: Scatter plots of the Niño3 SSTA on Day(-20) vs. the Niño3 DSSTA on Day(60) for (a) Type W, (b) Type C and (c) Type E WWEs, and (d) for periods without WWEs. The units are °C, the vertical lines indicate the boundaries of the Niño3 SSTA regimes (COLD, REG, WARM), and the horizontal green lines indicate the composite values inside the REG and WARM regimes. Red marks highlight WWEs whose wind measure exceeds  $1.5 \times 10^6 \text{ m}$ .

equatorial Pacific SSTA in the absence of WWEs are very different from those when WWEs occur. Most notably, in the REG temperature regime there is a much greater likelihood for warming following WWEs than in the absence of WWEs, and a corresponding decrease in likelihood of eastern Pacific cooling.

Table III.3 summarizes the percentage of events in the REG SSTA regime which were followed by Day (60) Niño3 SSTA changes in various ranges, for all three equatorial WWE types, for equatorial WWE types of strong intensity (wind measure statistic in excess of  $1.5 \times 10^6 \text{ m}$ ; HV97), and for non-event periods. Notice that the probability of extreme Niño3 warming following WWEs ( $>1.0^\circ\text{C}$ ) is between 10 and 15 times that in the absence

of WWEs; and there is a greater than 50% chance of moderate ( $>0.5^{\circ}\text{C}$ ) warming following strong WWEs. In addition, no strong equatorial WWEs were followed by cooling of more than  $-0.5^{\circ}$  (in Fig. 8 this relation is also evident), and a total of three weak WWEs (one Type E and two Type C) WWEs were followed by moderate cooling.

This observational study provides support to the previous model and theoretical suggestions that equatorial westerly wind events are a fundamental mechanism in the appearance and maintenance of warm eastern equatorial Pacific SST anomalies. In the absence of WWEs the tropical Pacific SST tends to return toward or remain at climatological values, in the presence of WWEs the evolution is quite different. When the eastern equatorial Pacific SST is close to climatological values, equatorial WWEs are associated with strong warming of the equatorial waveguide of similar amplitude and structure as that associated with the onset of El Niño conditions. When eastern equatorial Pacific SST was warmer than climatology, some WWE types were associated with maintenance of the warm eastern and central equatorial Pacific SSTA values. Given the agreement between these statistical results and previous modeling and theoretical work on ocean response to WWE forcing, I

TABLE III.3: Percentage of WWEs and non-event periods with Day (-20) NIÑO3 SSTA in the range  $\pm 0.75^{\circ}\text{C}$  which have NIÑO3 SSTA change on Day (60) in the ranges indicated. Strong events indicates WWEs whose wind measure (an indicator of WWE strength) exceeded  $1.5 \times 10^6$  m. Notice the considerable likelihood of NIÑO3 SSTA warming following equatorial WWEs.

WWE Type	Number of events	Percentage of REG events with Day(-60) NIÑO3 $\Delta$ SSTA in range:			
		$<-0.5^{\circ}\text{C}$	$>0.25^{\circ}\text{C}$	$>0.5^{\circ}\text{C}$	$>1.0^{\circ}\text{C}$
W	30		50	47	30
Strong W	13		62	54	38
C	38	5	63	39	32
Strong C	16		81	63	50
E	19	5	58	42	21
Strong E	5		80	80	40
In absence of equatorial WWEs		15	26	10	2

suggest that WWE driven warming of the central and eastern equatorial waveguide is a fundamental mechanism for the onset of warm El Niño conditions in the equatorial Pacific and in the maintenance of warm El Niño conditions in the equatorial Pacific.

In Chapter V the mechanisms responsible for the SSTA changes following WWEs are examined. The next chapter, Chapter IV, describes the relationship between WWEs and atmospheric convection, and between WWEs and certain atmospheric circulation patterns (tropical cyclones and the MJO), in order to further develop an understanding of the coupled mechanisms involved in the evolution of WWEs.